The Pulmonary Anatomy of *Alligator mississippiensis* and its Similarity to the Avian Respiratory System

KENT SANDERS[1]* AND C.G. FARMER[2]
[1]Department of Radiology, Musculoskeletal Division,
University of Utah Health Sciences Center, Salt Lake City, Utah
[2]Department of Biology, University of Utah, 257 S 1400 E, Salt Lake City, Utah

ABSTRACT

Using gross dissections and computed tomography we studied the lungs of juvenile American alligators (*Alligator mississippiensis*). Our findings indicate that both the external and internal morphology of the lungs is strikingly similar to the embryonic avian respiratory system (lungs + air sacs). We identified bronchi that we propose are homologous to the avian ventrobronchi (entobronchi), laterobronchi, dorsobronchi (ectobronchi), as well as regions of the lung hypothesized to be homologous to the cervical, interclavicular, anterior thoracic, posterior thoracic, and abdominal air sacs. Furthermore, we suggest that many of the features that alligators and birds share are homologous and that some of these features are important to the aerodynamic valve and are likely plesiomorphic for Archosauria. Anat Rec, 00:000–000, 2012. ©2012 Wiley Periodicals Inc.

Key words: alligator; lungs; pulmonary; anatomy; archosaur

INTRODUCTION

Crocodilians are the sole surviving members of pseudosuchia, a morphologically diverse and prominent clade of vertebrates that thrived during the Triassic Period (Sereno, 1991; Benton, 2004; Brusatte et al., 2008, 2010, 2010; Nesbitt, 2011), and are therefore the only extant lineage available for neontological studies that aim to elucidate the evolutionary history of this remarkable lineage. However, such studies need to distinguish between features that are adaptations of modern crocodilians, which are all semiaquatic predators, and features inherited from their ancestors, which occupied a range of guilds. During the Triassic there were herbivorous pseudosuchians, such as the aetosaurs, and giant carnivorous lines, including the rauisuchid and poposauroid archosaurs. There were also pseudosuchian lineages that occupied the same ecomorphological niches that would be filled later by ornithodiran archosaurs, which include the pterosaurs and dinosaurs. For example, *Effigia okeeffeae* resembled an ostrich (Nesbitt and Norell, 2006). Although initially more abundant and successful than ornithodiran archosaurs, all pseudosuchians were extinct by the end of the Triassic with the exception of a few lineages of crocodylomorphs. However, the earliest crocodylomorphs, the sphenosuchians, were very different from modern crocodilians. They were terrestrial, small (cat to greyhound sized), and had a parasagittal posture and numerous cursorial features: gracile limbs, digitigrady, and a reduced number of digits (Sereno, 1991; Benton, 2004; Brusatte et al., 2008; Brusatte et al., 2010). By the Early Jurassic, most crocodylomorphs had evolved a semiaquatic or marine lifestyle (Brochu, 2001). The crown group that includes all 23 extant species arose by the end of the Cretaceous (Brochu, 2003). The ecomorphological niche occupied by extant crocodilians, that is, relatively large and heavy bodied semiaquatic carnivorous or piscivorous ectotherms, belies the great diversity of their distant ancestors and could hardly be less similar to their extant sister taxon, the lightly built and endothermic birds. Although superficially birds and crocodilians have little in common, their cardiopulmonary systems are similar, particularly the embryonic forms (Locy and Larsell, 1916; Broman, 1940; Holmes, 1975; Seymour et al.,

Grant sponsor: NSF; Grant number: IOS-0818973; Grant sponsor: S. Meyer.

*Correspondence to: Kent Sanders, 50 North Medical Drive #1A71, Salt Lake City, UT 84132. E-mail: kent.sanders@hsc.utah.edu

Received 5 July 2011; Accepted 29 December 2011.
DOI 10.1002/ar.22427
Published online 00 Month 2012 in Wiley Online Library (wileyonlinelibrary.com).

2004), which may indicate that their common ancestors, basal archosaurs, were highly athletic animals (Farmer, 1999; Carrier and Farmer, 2000; Farmer and Carrier, 2000) but does not necessarily mean they were endotherms (Farmer, 2000, 2001, 2003), but see Seymour et al., (2004) for opposing view. Furthermore, it is possible these cardiopulmonary features are exaptations that facilitated the evolution of expanded aerobic capacities (Farmer, 2010). Conventionally, the avian lung + air sac system is viewed as a cornerstone for the renowned aerobic capacity of birds, and as a very derived and unique respiratory system (Maina, 2000, 2006). However, the discovery of unidirectional airflow in alligator lungs (Farmer, 2010; Farmer and Sanders, 2010) raises the possibility that many features are synapomorphic for archosaurs. It is not clear if unidirectional airflow is an exaptation, initially serving in cardiogenic flow during apnea (Farmer, 2010), an adaptation for expanded aerobic capacity during a time of environmental hypoxia, (Farmer, 2010; Farmer and Sanders, 2010), or if it serves another, unknown function. A more detailed understanding of the anatomical, developmental, and functional similarities of these respiratory systems is needed to shed light on this question.

Using computed tomography and gross dissections, we examined the anatomy of the alligator lung with the aims of gaining insight into the mechanisms by which this pattern of flow is generated and of elucidating pulmonary features that may be homologous with the avian lung + air sac respiratory system. Like previous workers (Huxley, 1882; Moser, 1902; Wolf, 1933; Broman, 1939; Boelert, 1942; Perry, 1988, 1989, 1990, 1992, 2001), we find a similar structural plan is present in the crocodilian and avian lung. We detail the macroscopic anatomy of the alligator lung, homologize avian similarities and identify various morphological characters that might be associated with unidirectional airflow. These include a Hazelhoff loop-like aerodynamic valve (Hazelhoff, 1951), dorsally located hypervascular gas exchange lung zones, nested spiral dorsal intrapulmonary conductive bronchi, ventral intrapulmonary bronchi, and hypovascular ventrally located regions within the lung that may be homologous with avian air sacs, and small diameter tubules that may be homologous with parabronchi.

MATERIALS AND METHODS

Our investigation included the gross inspection of fresh lungs *in situ* and *ex vivo*, as well as inflated dried specimens of *A. mississippiensis*. We imaged a live unsedated 11 kg alligator (snout to occipital condyle skull length 18.8 cm) during natural apnea using a 164 slice dual energy Siemens SOMATOM Definition computed tomography unit. Image acquisition parameters included: slice thickness one mm, kVp 120, MA 200. The one mm image data were filtered in soft tissue and lung algorithm while additional 0.6 mm image reconstructions were further edge-enhanced with a high-resolution lung algorithm. We used a Siemens Wizard workstation and proprietary software to make coronal and sagittal reconstructions and three-dimensional volume renderings including virtual endoscopy. Linear measurements were obtained from the DICOM data using Dicom Works v1.3.5 and Syngo Fastview. We used Amira 5, Mimics, Avizo image processing software to segment DICOM image files to generate three-dimensional models.

RESULTS

General Anatomy

An elongated trachea bifurcated into two nearly equal length primary bronchi whose intrapulmonary extensions were the only enclosed air conducting structures. The intrapulmonary primary bronchi were short and heavily fenestrated with three distinct forms of ostia: (1) a conical ostium to the cervical ventral bronchus (CVB); (2) large and flush bronchial macroostia leading to hypervascular regions; and (3) submillimeter ventral microostia associated with hypovascular air storage spaces. There were eight large secondary bronchi that were associated with the hypervascular lung. These included two dorsomedial bronchi (DMBs), a single large dorsolateral bronchus (DLB), and five caudal bronchi that originated at or near a common passageway formed at the caudal terminus of the intrapulmonary bronchus. These five together constituted the caudal group bronchi (CGBs). There were three cervical ventral secondary bronchi that extend along the hypovascular ventral lung cranial to the primary bronchus. The main cervical ventral bronchus (CVB) extended from the lung apex to the primary bronchus (Fig. 1) while the smaller and more F1
ventrolateral accessory bronchi extended for less than half that length, originating on a common ostium of the ventrolateral wall of the conical ostium of the main CVB (Fig. 12). The hypervascular bronchi, with the exception of the diminutive caudal branch of the DMBs that projected caudomedially, spiraled toward the lung apex and in turned to give rise to a spiral pattern of tertiary bronchi. The tertiary bronchi in turn appeared to give rise to identically arranged air exchange tubules, thus constituting a fractal growth geometry referred to as "spiral turbinal geometry." The CVBs were ventral to hypervascular tertiary bronchi. The parenchyma between the hypervascular bronchi and CVBs were the apicoperipheral convergence zone and were characterized by a ventrolateral manifold of collection tubes emptying primarily into the main CVB and the saccular lung apex. Ventromedially the walls and lumen of the CVBs gave rise to relatively larger hypovascular and somewhat honeycombed saccular cavities, also in spiral pattern that were lined by large draining veins. The pulmonary vascular system followed the interbronchial parenchymal septations. The vessels were named therefore for their bronchial associations. In general large arteries were dorsal and relatively peripheral while large veins were ventral and medial. The lungs were conical in shape with a narrow apex and broad base. Both were nearly equal in volume. The hypervascular gas exchange parenchyma was dorsolaterally located, while the hypovascular lung was located ventrally, forming a gas storage space (intrapulmonary air sacs). These air sacs communicated with the bronchi and intrapulmonary bronchus primarily through ventral microostia.

Trachea

From its first subglottic tracheal ring to the apex of the carina, the undivided trachea of the 11 kg animal measured 20.7 cm during apnea. Dorsal longitudinal

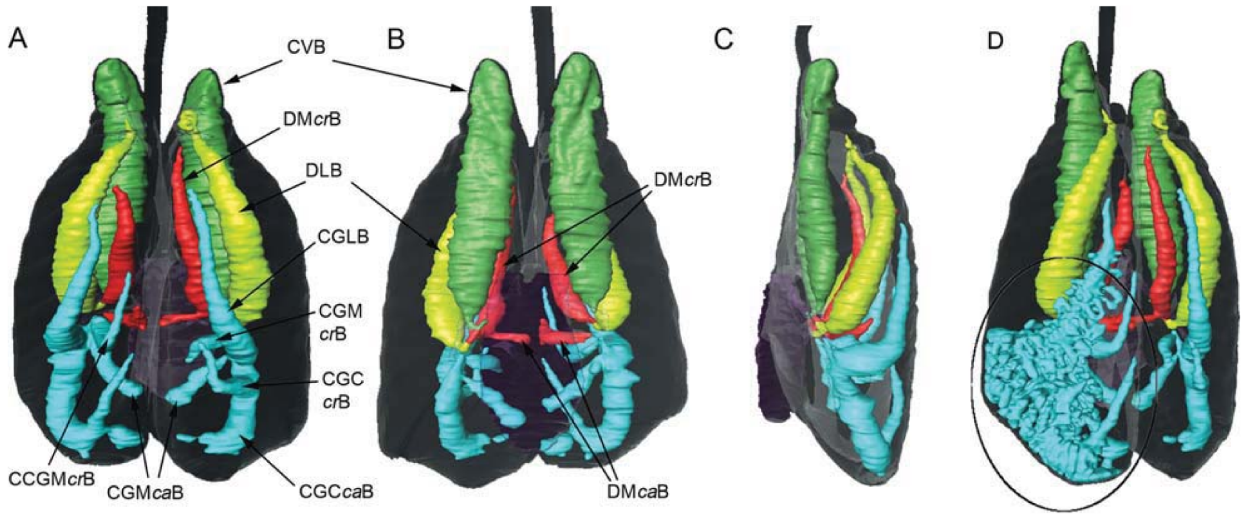

Fig. 1. (**A–D**) show dorsal, ventral, left lateral, and left dorsolateral 3D representations of the major secondary bronchi. The cervical ventral bronchi (CVBs) are colored green, the dorsolateral bronchus (DLB) is chartreuse, the two dorsomedial bronchi (DMB): the cranial (DM*cr*B), and the caudal (DMcaB) are red, the five caudal group bronchi (CGB): the lateral (CGLB), caudal cranial (CGC*cr*B), caudal (CGC*ca*B), medial cranial (CGM*cr*B), and medial caudal (CGM*ca*B) are light blue. Note in 1C how the main CVB is located cranioventrally and how the hypervascular bronchi originate ventrally and spiral craniodorsally. The circled area in 1D shows how the included tertiary bronchi arising from the CGLB and CGC*ca*B fill the dorsolateral, hypervascular lung.

folds converged sagittally and slightly protruded into the dorsal lumen in the cranial-most 3.7 cm of the trachea just ventral to hypopharynx. The cross-sectional shape in the cranial half of the trachea was a dorsoventrally flattened oval that tapered from the subglottic maximum diameter of 18.1 mm transverse by 16.7 mm AP, to a mid-tracheal maximum flattening of 10.8 mm transverse by 5.8 mm AP. The caudal half of the trachea, beginning at the level of the lung apex and extending to the carina, was essentially circular in cross-section and measured 7.3 mm transversely by 7.1 mm AP. The carina overlayed the sagittal plane of the chest and was slightly dorsally displaced by the more ventrally located supracardiac confluence of the great vessels.

Primary Bronchi

The primary bronchi were anatomically divided into the extrapulmonary bronchi and their intrapulmonary extensions, and were the only intrapulmonary bronchi that were supported by cartilaginous rings. Only the proximal part of the intrapulmonary portion of the bronchus was cartilaginous; this portion accounted for approximately half the length of the total primary bronchus. The tracheal bifurcation formed a 90-degree angle of divergence in the coronal plane. The carinal fold sharply divided the bifurcation along the caudal surface. The left primary bronchus was more steeply angled from the sagittal plane forming an angle of 50–55 degrees while the right was slightly shallower at 35–40 degrees. Both were angled dorsally at about 25 degree from the coronal plane. The primary bronchi were short in length measuring 3.7 cm on the left and 3.9 cm on the right. The diameters were nearly uniform in the proximal three quarters of their length with roughly circular cross-sections measuring three mm in diameter. The terminal quarter of the intrapulmonary bronchi flared slightly into a common large diameter passageway or vestibulum that led to the CGBs. There were three distinct morphologies of primary bronchial ostia in addition to the caudal vestibular opening. Two types of large ostia included the conical and cranially directed CVB ostium, and the flush more dorsally directed bronchial macroostia. These were over two mm in transverse diameter and, in the case of the latter, were as long as 4 mm. The ostia of the third group were small at one to 0.5 mm in diameter and proximally were ventromedially directed while distally they were ventrolaterally directed. All were associated with hypovascular ventral air storage spaces (intrapulmonary air sacs), (Fig. 2). F2

The conical opening to the main CVB may be a key structure that creates a Hazelhoff loop-like aerodynamic valve that facilitates the unidirectional flow of air within the lung during the respiratory cycle (Hazelhoff, 1951). It was the first large ostium and was located 2.6 and 2.77 cm from the carina on the left and right, respectively. Its anterior primary bronchial opening measured 2.8 mm transversely by 2.2 mm AP. Unlike the other macroostia, it had walls that continue for a short distance into the main CVB to form a 5-mm long, rapidly expanding cone whose central axis formed an angle with the primary bronchus of ~70–75 degrees, with the medial and lateral walls of the cone forming angles of 59–85 degrees from the long axis of the anterior primary bronchus in the coronal plane. A ventrolateral, periconal ostium was just lateral to the pulmonary artery and projected cranially into a common opening of two ventrolateral accessory CVBs. A sheet of parenchymal connective tissue separating the two structures had the potential to form a flap valve against the pulmonary artery (Fig. 3A–C). F3

From the CVB ostium to 5 mm into the main CVB, the cross-sectional area of the cone expanded from 4.84 to

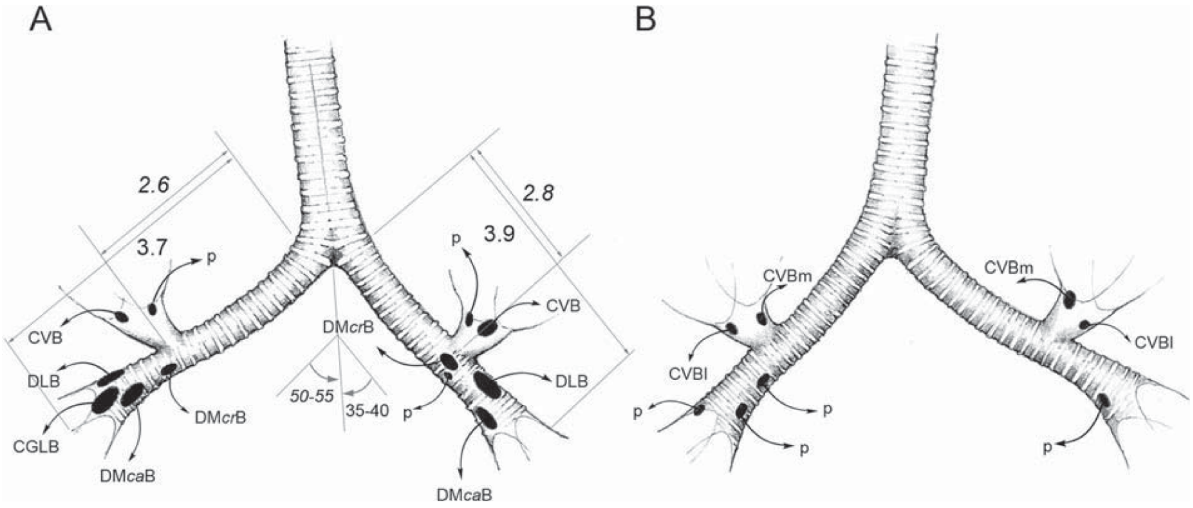

Fig. 2. Schematic of the primary bronchi and the openings into the secondary bronchi in dorsal (**A**) and ventral (**B**) views. Ostia on the CVB cone are variable. Lettering as in Fig. 1.

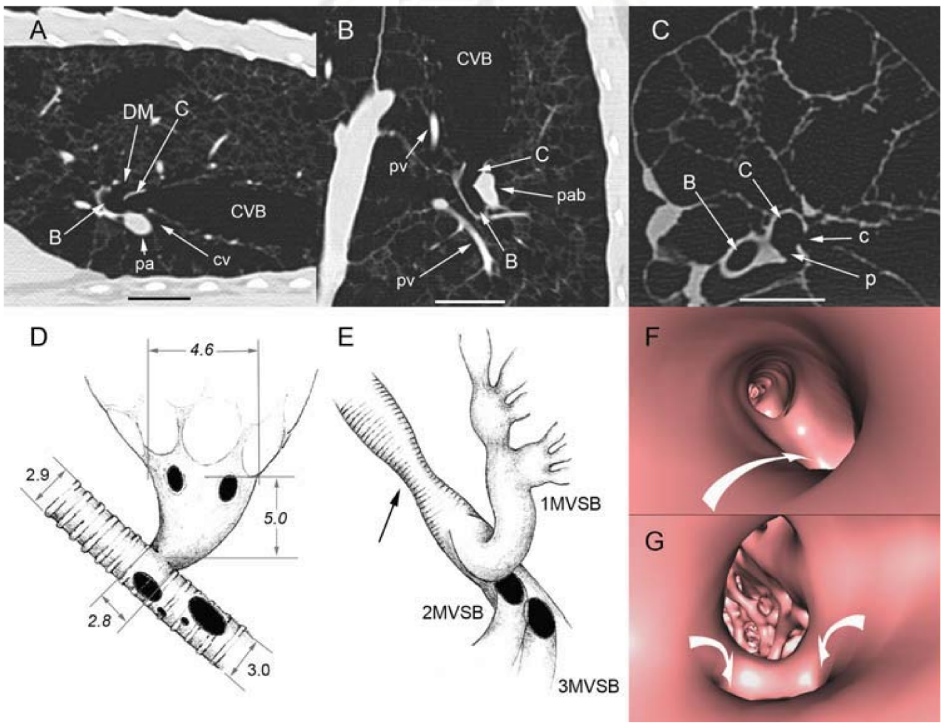

Fig. 3. Sagittal (**A**) and coronal (**B**) 1-mm high-res CT of main CVB periconal ostia in a live alligator. The conical CVB ostium opens cranially into the main CVB above a periconal ostium into the medial cranial air sac. The floor of the conical ostium (**C**) is in proximity of the pulmonary artery (pa) creating potential valve (cv). In the coronal image (B) cranial is up. The cone is laterally bounded by the pulmonary artery bifurcation (pab). Figure 3C is a 0.6 mm transverse high-res CT of an explanted inflated lung at the cranial margin of the cone—medial is left. Two ventral periconal ostia open into the cranial and pericardiac (p) air sacs. Other abbreviations: pv—pulmonary vein, B—primary bronchus, DM—ostium to DMB. Scale bars = 2 cm. Figure 3**D**,**E** shows a dorsal schematic of the right primary bronchus in the alligator (C) and chicken (D). The alligator bronchus lacks the constricted segmentum accelerans (arrow in D) proximal to the conical ostium of the main CVB. A similar but more exaggerated configuration is seen in the hairpin turn of the first medioventral secondary bronchus in the chicken (1MVSB). (**F**) Virtual endoscopy looking caudally down the alligator primary bronchus. The arrow indicates the conical ostium and approximates the direction of the view in **G**. Arrows in G show the periconal ostia c and p with the lumen of the CVB in the distance cranially.

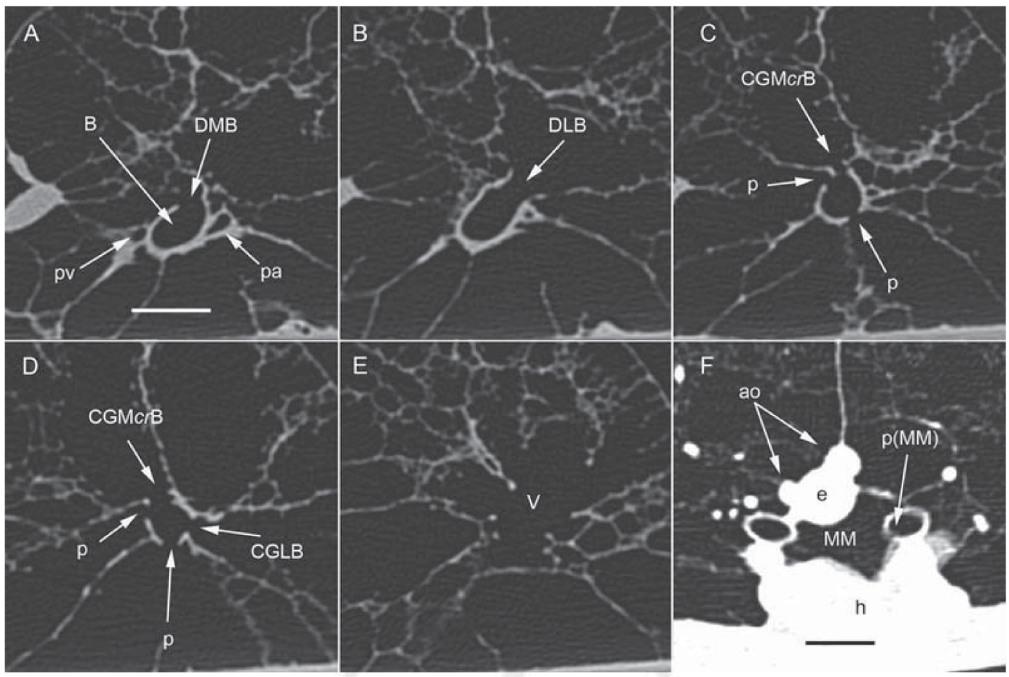

Fig. 4. (**A–E**) are transverse 0.6 mm CT sections of an inflated explanted lung. The upper right hand corner is dorsal, left is medial. Images are centered on the mesobronchus (B) and begin at a location just caudal to the main CVB ostium, and progress caudally to the vestibulum of the CGBs (V). The macroostia are denoted by the abbreviations for their respective IPBs. Microostia of the caudal pericardiac air sacs are marked "p." The pulmonary vein (pv) and artery (pa) are air-filled and partially collapsed. (**F**) is a transverse 1-mm CT section of a live alligator just below the carina. Blood-filled vessels are white and distended. A microostium to the right intercalvicualr mesial moiety arises from the right bronchus and is marked MM. The mesial moiety is between the heart (h) and the esophagus (e) and paired aortas (ao). Scale bars = 1 cm.

12.64 mm^2. At 11.6 mm from the ostium, the main CVB cross-sectional area ballooned to 84.8 mm^2. The recurved geometry of the conical expiratory ostium (Fig. 3D) was distinctly similar to the proximal bend of the first medioventral secondary bronchus (entobronchus) described in birds. During apnea, and at the spatial limitations of our ability to measure distance by CT (roughly ± 0.1 mm), the cranial intrapulmonary bronchus did not appear to constrict near the ostium of the CVB in the form of the segmentum accelerans as seen in most birds (Fig. 3E). Maina (2001) reported that the segmentum accelerans "may be generally lacking" in ratites also and is not a necessary component of the aerodynamic valve of flightless avians.

The macroostia were relatively large and occurred in clusters that corresponded to the bronchi that they supplied. The more cranially located macroostia were also generally smaller than the caudally located ostia. The first macroostium led to the two DMBs, the next to the large singular DLB, and the last dorsal cluster to the dorsal branches of the CGB. The primary bronchial vestibulum formed a short passageway for the common
F4 origin of the remaining CGB (see Fig. 4A–E, CT transverse sections of ostia). The small ventromedial bronchial microostia appeared as discrete millimeter–submillimeter bronchial wall openings leading to medial pericardial air sacs (see Fig. 4C–F).

Secondary Hypervascular Bronchi

Of the eight secondary hypervascular bronchi, the DLB was the largest, both in overall length and diameter, and was the simplest in morphology (Fig. 1A,C,D). It also extended farthest into the lung apex. It was positioned between the remaining hypervascular bronchi and the main CVB. The cranial DMB was the larger of the DMBs and was the most medially of all the hypervascular bronchi. The caudal DMB was the smallest of the hypervascular bronchi and laid most closely to the pericardiac air sacs. The CGBs and their respective hypervascular parabronchi filled the caudal half of the lung (Fig. 1A–D) and appeared most affected by diaphragm motion (Fig. 5).
F5

The five branches of the CGBs were: two small medial (cranial and caudal) branches, a large singular lateral branch, and a pair of caudal branches that were also arranged as a craniocaudal bifurcation. As with the previous hypervascular bronchi, the CGBs spiraled at a high pitch (large longitudinal travel per rotation) from their ventral origin dorsomedially to their cranial terminations. The lateral CGB reached apically the farthest. The bifurcation of the caudal branches was more caudal/terminal in location on the left (Fig. 1A labeled in the right lung as CGC*cr*B and CGC*ca*B). The middle segment of the primary bronchus was marked by a slight luminal expansion that also gave rise to laterobronchi (discussed below).

Each hypervascular bronchus had a similar architecture in which the tertiary bronchial openings were arranged in a low-pitch spiral pattern along the lumen of the bronchus. The lumens of the tertiary bronchi were subsequently arranged in a radial spiral pattern from the lumen of the respective bronchi. The arrangement of

J_ID: Z3X Customer A_ID: 11-0185.R1 Cadmus Art: AR22427 Date: 8-February-12 Stage: Page: 6

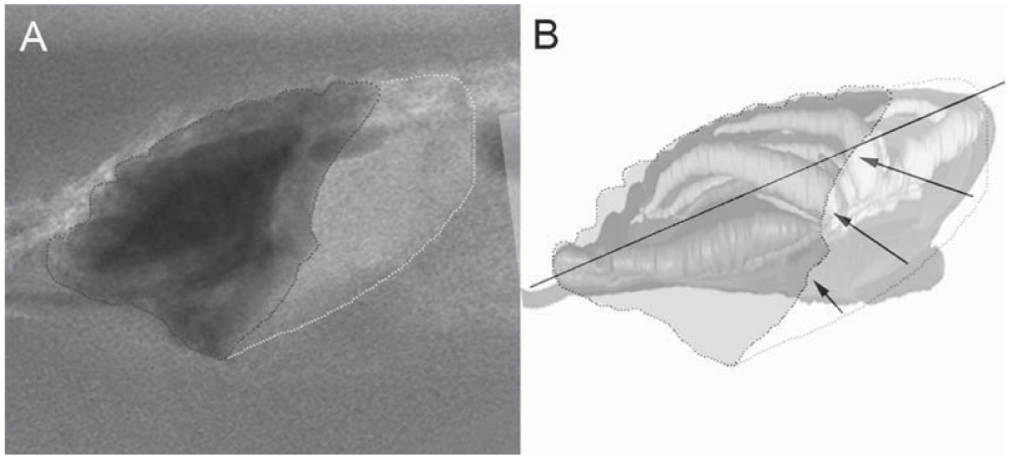

Fig. 5. (**A**) Superimposed fluoroscopic images of lung volume changes in a floating hatchling alligator in left lateral view. Full inspiratory lung volume is outlined in white, while predive full expiratory volume is outlined in black. (**B**) A diagrammatic image of (A) with a lung overlay. The line represents the anatomic coronal plane and arrows indicate the direction and magnitude of craniodorsal liver/diaphragm motion with compression of the CGBs and caudal air sacs.

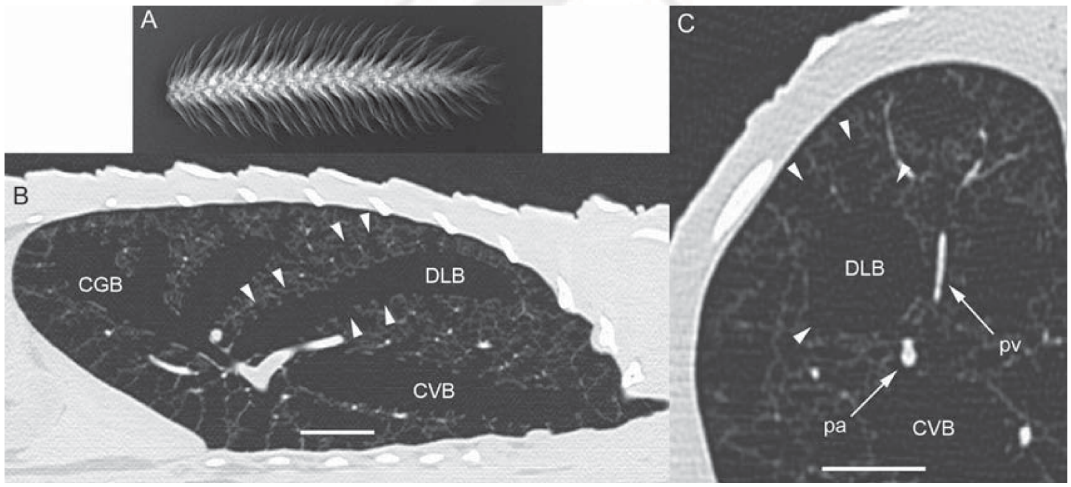

Fig. 6. (**A**) Radiograph of a spruce cone. The core of the cone is analogous to the lumen of the secondary bronchus and the scales arise in a spiral pattern from the core and are inclined toward the apex of the cone similarly to tertiary bronchi. (**B**) Parasagittal CT image of an alligator right lung (during full inspiration) through the central long axes of the DLB and main CVB. Arrowheads indicate several tertiary bronchi extending from the DLB. Note that the camerae of the main CVB are more inclined toward the apex than those of the DLB at full inspiration. (**C**) Transverse section of the right mid-lung showing the spiral radial orientation of the DLB tertiary bronchi (arrowheads). Scale bars = 2 cm.

the tertiary bronchi along a hypervascular bronchus was architecturally and mechanically similar to the scales of a pine cone (Fig. 6A–C). The change in volume of a bronchus and its tertiary bronchi during inhalation and exhalation may be achieved in the same manner as the change in volume of a pine cone when its scales are opened verses closed. The central axes of the tertiary bronchi were variably inclined toward the apex relative to the long axis of the bronchus depending on the degree of lung inflation. When the lung was fully inflated, the tertiary bronchial axes were relatively obtuse and their lumens were distended. When the lung was deflated, the tertiary bronchial axes were relatively acute and their lumens were collapsed (Fig. 7). The parenchymal interfaces of the stacked tubular bronchi when viewed in cross-section formed bronchial domains with the lumen and luminal draining spiral veins at the center. The tertiary bronchi were arranged radially from the bronchial lumen. The larger intrapulmonary blood vessels were located in the peripheral corners. Tertiary bronchial arterial blood flow appeared to be centripetal and opposite to the expected airflow in the tertiary bronchus (Fig. 8).

Tertiary Bronchi

Tertiary bronchi constitute the macroscopic respiratory functional unit of the lung analogous to mammalian terminal pulmonary lobule. They were architecturally similar to their parent hypervascular bronchi and formed the third generation of the fractal spiral turbinal

ID: kalas | Black Lining: [ON] | Time: 14:00 | Path: N:/3b2/AR##/Vol00000/120027/APPFile/JW-AR##120027

morphology. Small air diverticula were arranged in a spiral pattern around the lumens of the tertiary bronchi. The fibrovascular cores of the tertiary bronchi when sectioned longitudinally revealed the familiar pine cone-like spiral motif (Fig. 9A). The air diverticula that lined the bronchi appeared to arise serially in spiral pattern. The terminal diverticula in the periphery of the tertiary bronchi interdigitated with diverticula of adjacent tertiary bronchi. These terminal diverticula were sometimes fenestrated at their tips so that air from IPB domains might move into neighboring domains as it travels cranially through the hypervascular lung (Fig. 9B,C).

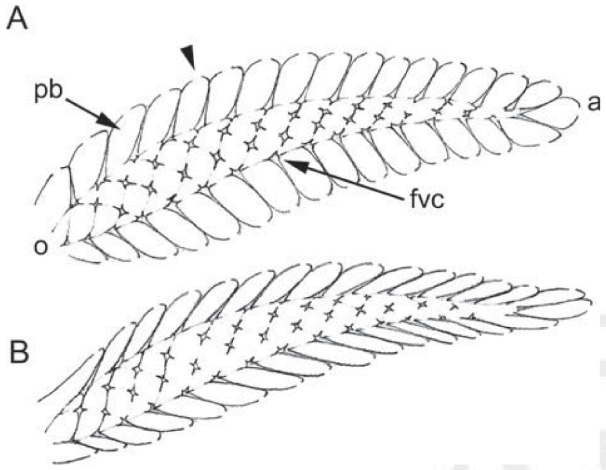

Fig. 7. (**A**,**B**) Diagrammatic representation of the DLB and its volume change between full inspiration (A), and modest exhalation (B). The bronchial ostium (o) at the base is caudal and the luminal apex (a) is cranial. Note the change in inclination of the fibrovascular cores (fvc) that form the walls of the tertiary bronchi (b) and the subsequent decrease in their volumes and overall bronchial diameter with exhalation. The arrowhead indicates one of many terminal openings of the tertiary bronchi that could provide cranial air flow with exhalation.

Apicoperipheral Convergence Zone

As shown previously, the cranial extent of the hypervascular bronchi converged toward the apical and subpleural peripheral lung. The lung parenchyma here was hypovascular with cavities that formed somewhat sequentially along the subpleural lung, growing larger and coalescing toward the apex. The apex of both lungs was characterized by a cavity from which arose the cranial end of the main CVB, as well as the most cranial extent of the ventrally located intrapulmonary air sacs. This cavity marked the convergence zone for air expelled from the craniodorsal hypervascular part of the lung. Figure 10 shows selected CT images of lung apex revealing the relationship of the apical extent of the DMcrB and DLB and the apical convergence zone with the cranial extent of the main CVB. Tertiary branches from the DLB extended obliquely through the dorsolateral hypervascular lung and contributed to the manifold-like connection to the cranial part of the main CVB.

Cervical Ventral Bronchi

The main CVB was between the craniodorsal hypervascular lung and the hypovascular ventrally located intrapulmonary air sacs. Its morphology differed from the hypervascular bronchi in that the lumen was more uniform in diameter rather than continuously tapering, and it was not spiral in shape. Its lumen gave rise to fewer and larger diameter hypovascular cameral side projections whose openings were arranged along a spiral course. The projections of the main CVB extended to the

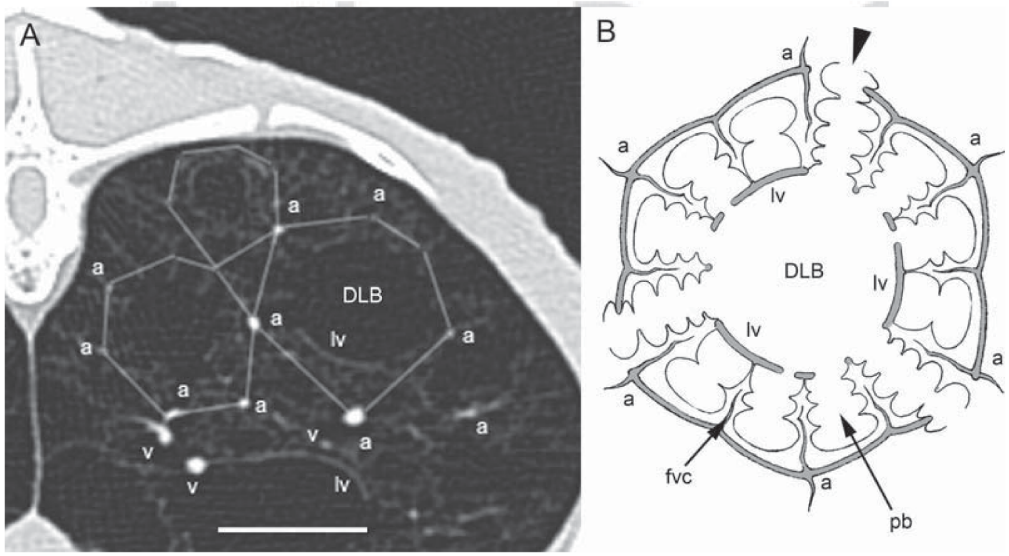

Fig. 8. (**A**) 1-mm transverse CT image of a live alligator with lines connecting the bronchial arterial branches to outline polygonal bronchial vascular domains. (**B**) Simplified transverse diagram of a single vascular domain. Precapillary arteries (a) are located in the periphery while postcapillary veins (lv) line the lumen. Arteriolar radicals form the fibrovascular cores (fvc) of the parenchymal septa separating the tertiary bronchi (pb). The arrowhead indicates one of the terminal interbronchial openings. Conducting pulmonary veins (v) travel to the heart ventral to the hypervascular lung.

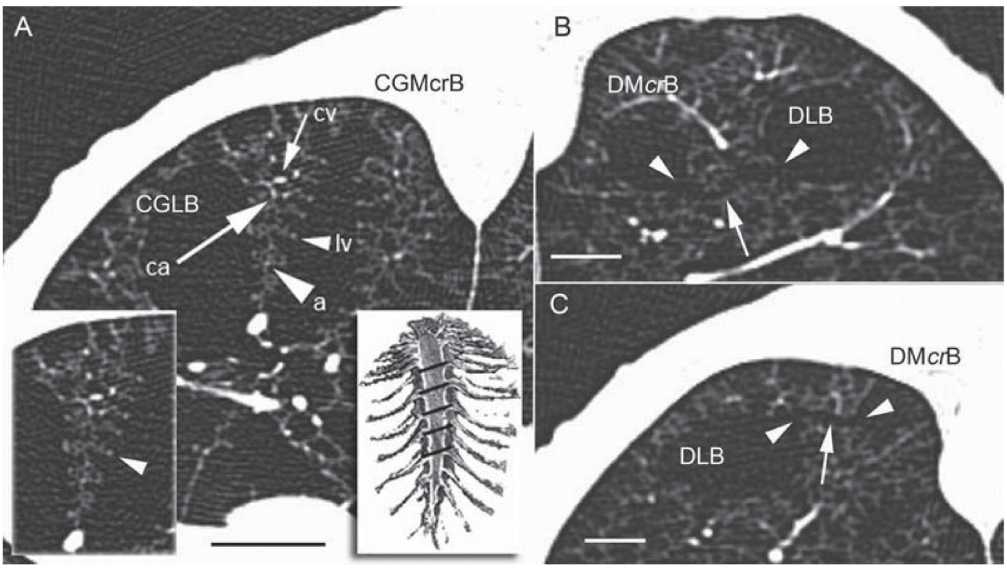

Fig. 9. (**A**) 0.6-mm transverse CT image from the caudal left lung showing the fibrovascular parenchyma separating the CGLB and CGMcrB; the lower left inset is the same structure. The small arrowhead points to the repeated spiral fractal geometry in a single interbronchial septum. The lower right inset is a sectioned pinecone oriented similarly with black bars indicating the spiral pitch. Its scales are analogous to interbronchial septa. Conducting arteries and veins (ca and cv) are located along the interbronchial interstitial core. Conducting arteries give rise to arterioles (a) that branch from the core into each of the interbronchial septa where gas exchange occurs. Postcapillary blood drains into the luminal veins (lv). Scale bar = 2 cm. (**B**,**C**) Transverse sections through the right and left lungs respectively, showing terminal interbronchial communications (arrows) between the labeled bronchi. Arrowheads mark the tertiary bronchial openings. Scale bars = 1 cm.

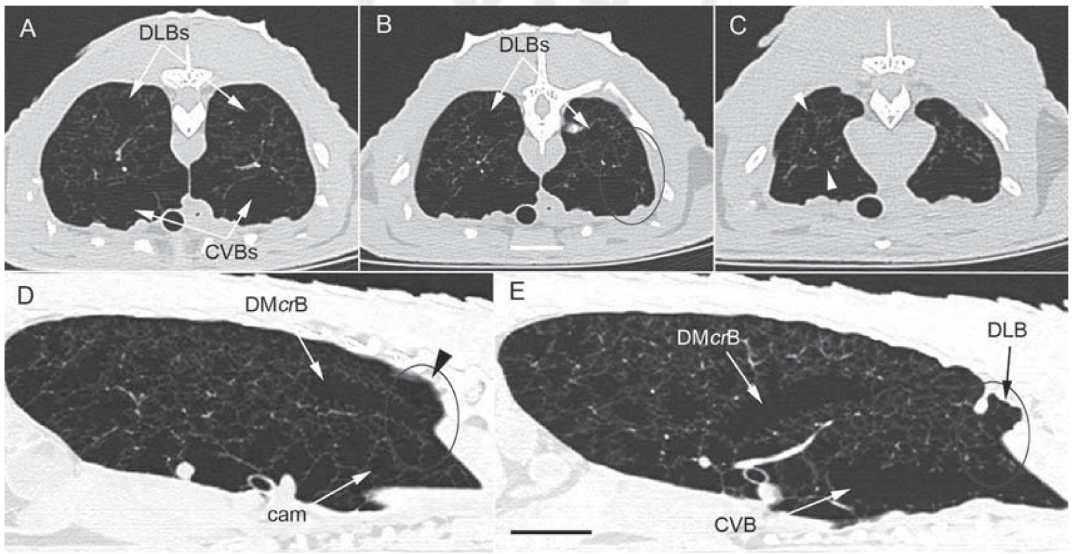

Fig. 10. (**A**–**C**) Serial 0.6-mm transverse CT images of a live alligator through the apical lung between the origins of the DMcrB and DLB. Images progress cranially. Scale bar = 2 cm. The lung parenchyma becomes sparser and the tertiary bronchi appear to coalesce with peripheral subpleural spaces (oval in B). Arrowheads in (C) show a direct tertiary bronchial communication from the terminus of the left DLB and the apex of the main CVB. (**D**,**E**) Sagittal CT sections of the same animal located along the medial edge of the main CVB. The oval in (D) shows the terminus of the DMcrB and its juxtaposition to the medial paraspinal apicoconvergence zone (arrowhead). The main CVB camerae (cam) are located immediately ventrally. (E) is located lateral to (D). The oval indicates the terminus of the DLB and its similar association with the camerae. The DLB arrow shows the approximate location of 10C. Scale bar = 3 cm.

ventral and medial pleural surface of the lung cranial to the primary bronchus. In their medial and lateral extensions they formed a row of manifold-like projections that interdigitated with the tertiary bronchi of the nearest hypervascular bronchus. In this manner, the apicoperipheral convergence zone was extended throughout the

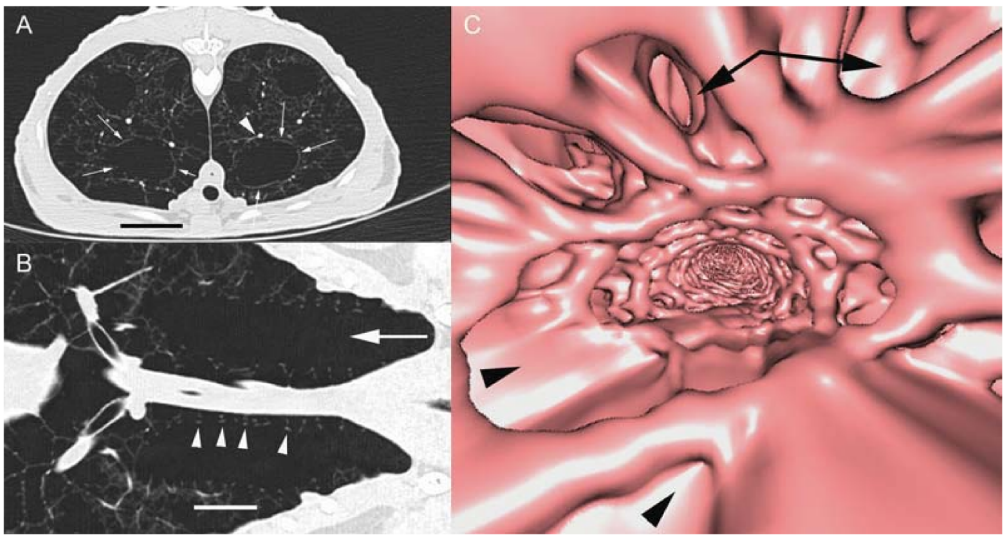

Fig. 11. (**A**) Axial CT image made from three combined 0.6-mm CT images showing a ring of luminal veins (arrows) outlining the main CVB. Arrowhead shows a venous radical entering the ventromedial branch of the right cranial pulmonary vein. (**B**) Coronal cross-section made from the same CT images as in (A). Arrowheads point to the same luminal veins in the coronal cross-section, arrow shows the caudal direction and approximate location of (**C**). Cranial is to the right, Scales bars = 2 cm. (C) The virtual endoscopic view shown by the arrow in (B); note the venous spiral arcades receding caudally in a counterclockwise direction. Arrows mark the lumens of dorsally projecting tertiary bronchi. Arrowheads mark the entrance of subpleural communications from the apicoperipheral convergence zone.

periphery of the apical lung (Fig. 10D). The smaller accessory CVBs had a similar but much more diminutive morphology and were more associated with the adjacent ventral intrapulmonary air sacs.

The luminal margins of these cameral projections were bounded by draining veins that formed a lattice F11 pattern along the CVBs lumens (see Fig. 11A–C). The floor of the proximal half of the main CVB contained large pulmonary veins that ran in a partial septum that separated the majority of the lumen from underlying ventral intrapulmonary air sacs and camerae that otherwise communicated with the main CVB by the apicoperipheral convergence.

Hypovascular Cranial Intrapulmonary Air Sacs

The ventromedial part of the lung was distinctly hypovascular with many relatively large cameral spaces divided by thin parenchymal septa. The primary bronchial microostia that communicated with these air sacs were ventrally located and smaller in diameter than the more dorsally directed macroostia. The air sacs were regionally, and probably functionally, divided into three groups: the cranial, pericardial, and caudal groups (Fig. 12A). The cranial group consisted of ventral camerae that arose from the ventral lumens of the CVBs caudal to the apicoperipheral convergence zone. The largest of these spaces was an air sac cavity that arose from the base of the medial accessory CVB and abutted the lateral ventral surface the anterior primary bronchus. The pericardial air sacs were those that contacted the pericardial mediastinum and included dorsal pericardial air sacs. These air sacs partially encircled the anterior primary bronchus along with the more laterally positioned lateral moiety (Fig. 12C,D). The right medial moiety had a primary bronchial ostium as well as a DM*ca*B ostial communication. There were smaller ventral and more caudally arrayed cameral projections that attached to the pericardial pleural reflection. The dorsal pericardial air sac was ventilated from the right side and was invested by the right pleura (Fig. 13). F13

Hypovascular Caudal Intrapulmonary Air Sacs

The caudal air sacs were ventrolaterally directed cameral projections that arose opposite the ostia to the CGBs (Fig. 14). In aggregate, they lined the entire ventrolateral lung caudal to the heart. There were two banks of camerae extending caudally and roughly parallel to the posterior pericardial camera. The more medial of these appeared to communicate with the posterior medial CGB and possibly the pericardial air sac associations with the DMcaB. Their primary communications were with their parent CGBs, with fewer terminal interconnections. The lateral bank camerae opened toward the lateral members of the CGB. F14

Pulmonary Arterial Anatomy

There were three small direct branches from the pulmonary arteries in addition to the two major trunks that supplied the majority of the lung. The small direct branches included two cranioventral branches that were the first pulmonary artery branches and supplied the CVBs. The larger of these two was the medial branch. Both traveled in the fibrovascular parenchyma separating the CVBs from the adjacent cranial air sacs camerae. The third direct pulmonary artery branch was a small medially directed pericardial air sac branch that arose from or just proximal to the mesial surface of the

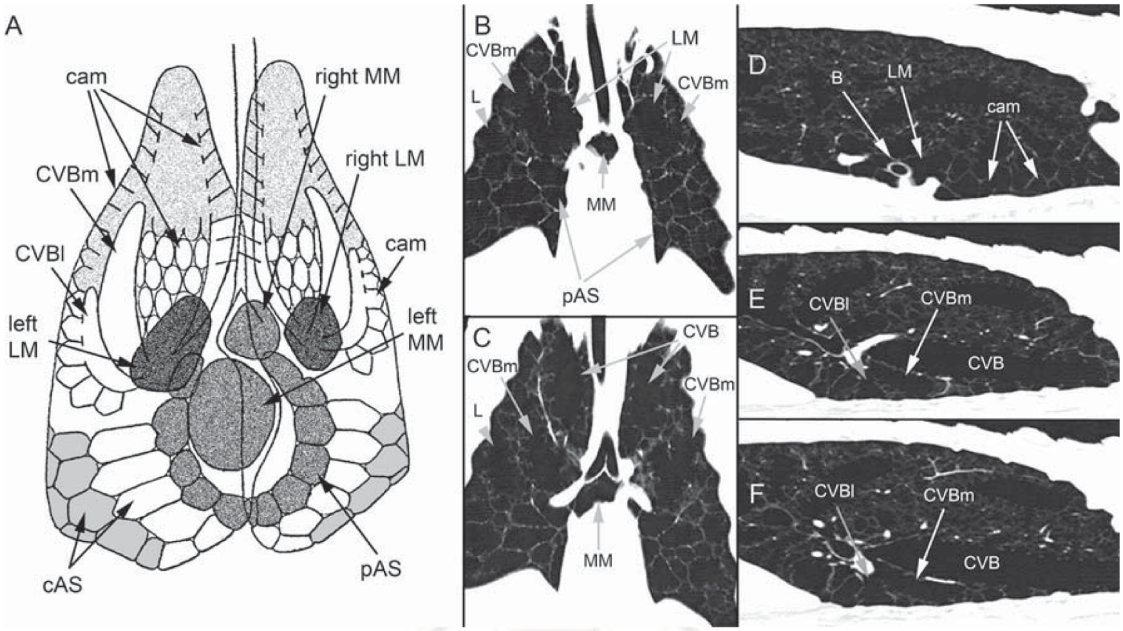

Fig. 12. (**A**) Simplified ventral air sac scheme where the dark stippled interclavicular lateral moiety homologues (LM) lay ventral to the medial CVB (CVBm). These, with the lateral CVB (CVBl) and their adjacent camerae, make up the cranial group of air sacs. The medium stippled pericardial air sacs include the left and larger right interclavicular mesial moiety homologues (MM) and the more caudal cameral pericardial air sacs (pAS). The latter share a common origin with the medial bank of white caudal air sacs (cAS) and as such may reflect a primordium of an anterior thoracic air sac system. The gray lateral cASs have a common lateral bronchial association and may reflect a posterior thoracic air sac system. The light stippled ventral apicoperipheral convergence zone is included for reference. Camerae (cam) form the medial and lateral manifold part of the apicoperipheral convergence zone as well as ventral air sacs of the CVBs. (**B**,**C**) Sequential coronal CT images showing the relationship of the CVBs to the more ventral medial LM, and the association of the LM and MM to the primary bronchus. (C) is dorsal to (B); cranial is toward the top of the page. (**D**,**E**) Sagittal CT images moving from the medial edge of the CVB in D to its center in **F**. The LM is medial to the CVBm and cranial (to the right) to the primary bronchus (B).

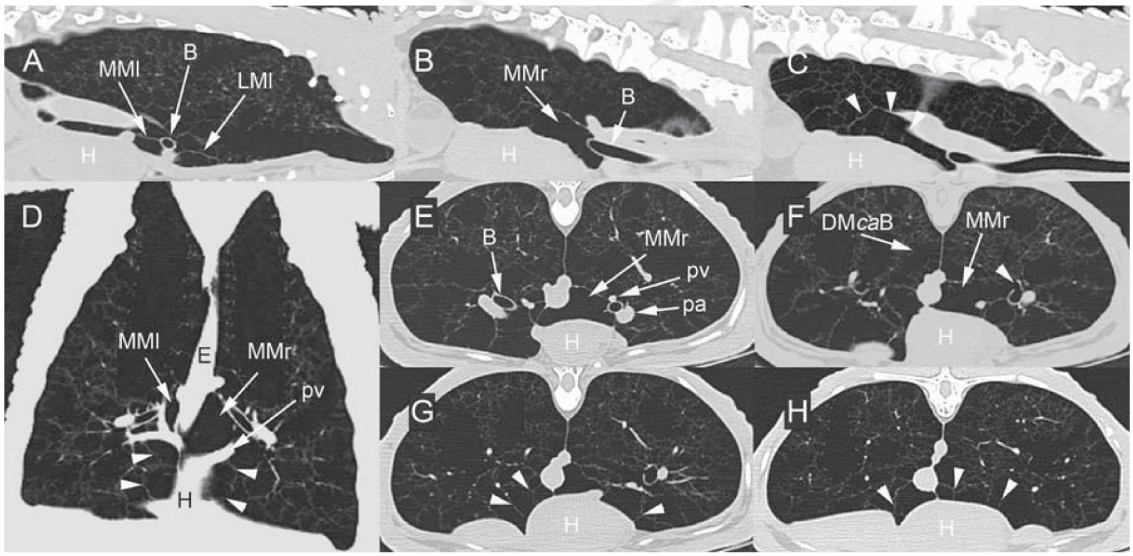

Fig. 13. CT images of living alligator. (**A**–**C**) Parasagittal CT images with the head to the right of the page. (A) A parasagittal section through the medial left lung showing the left mesial (MMl) and lateral (LMl) moieties surrounding the anterior mesobronchus. (B) is a right medial parasagittal section showing the larger right mesial moiety (MMr) and its relationship to the majority of the dorsal surface of the heart (H). (C) shows the more caudal ancillary pericardial camerae. Arrowheads indicate the divisions of these camerae. (**D**) Coronal image dorsal to the heart; head is at the top. (**E**–**H**) Serial axial images starting from the base of the cardiac vascular pedicle and progressing caudally. Arrowhead in (F) shows the ostium to the right DMcaB and the adjacent MMr. Arrowheads in (G–H) show how the caudal row of pericardial camerae are arranged toward the dorsal aspect of the heart.

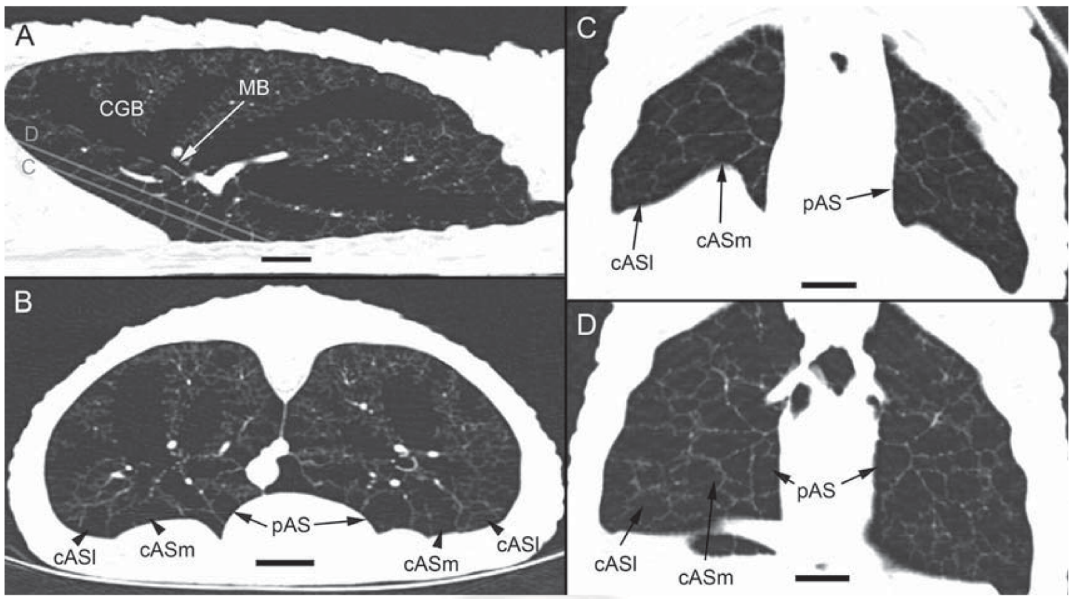

Fig. 14. (**A**) Parasagittal CT image showing the ventral posterior position of the caudal air sacs and their relationship to the CGB. Cranial is to the right. Lines C and D correspond to the coronal oblique CT reconstructed images in (**C**) and (**D**). These combined with the axial CT image in (**B**) show the medial (cASm) and lateral (cASl) rows of caudal air sacs. Note in (B) how the each row radiates from the mesobronchus (MB) extension into the CGB with the cASL row projecting laterally and the cASm positioned between the former and the pericardial air sacs (pAS). Scale bars = 2 cm.

pulmonary artery bifurcation. These pericardial vessels were more elaborate on the right, mirroring the asymmetry in pericardial air sacs.

The main right and left pulmonary arteries bifurcated F15 into cranial and caudal trunks (Fig. 15A). Subsequent branches reflected the bronchial anatomy with the arteries travelling in the fibrovascular interstitial cores of the lung parenchyma that formed the boundaries between the bronchi. The peripheral pulmonary arterial branches supplied multiple adjacent bronchi. In general, major branches of the parenchymal arteries were located dorsally in the lung within the hypervascular gas exchange zones. The right and left lungs had similar branching patterns with the relative lengths of particular vessels being the only difference (Fig. 15A).

The first cranial bifurcation was between the cranial trunk medial bronchial group and the dorsal lateral group. The dorsal lateral group was shorter and supplied the proximal part of the DLB and middle and terminal part of the dorsal lateral segment of the CGBs. The craniomedial branch of the cranial trunk also bifurcated, forming a ventromedial branch and a dorsal branch between the roof of the main CVB and the floor of the DLB. These supplied the middle and cranial part of the segments of the DLB and the cranial branch of the DMBs, as well as the majority of the main CVB. Terminal arterial branches to the latter appeared far fewer.

The caudal pulmonary artery trunk had many more branches reflecting the greater number of caudal and middle bronchi. In the single animal CTed for pulmonary vascular anatomy, the right caudal trunk was several millimeters longer than the left. The caudal trunks divided into medial and lateral branches, which subsequently divided into cranial and caudal peripheral branches. The medial branch supplied the caudal branch of the DMBs, caudal air sacs, and paired CGMBs and terminal CGCB. The lateral caudal trunk branch supplied the proximal CGLB and CGCBs, and the lateral row of caudal air sacs.

Pulmonary Venous Anatomy

The pulmonary venous system was more asymmetric in its branching pattern than the arterial anatomy (Fig. 15A,B). The pulmonary veins bifurcated very close to the left atrium into cranial and caudal trunks. The proximal pulmonary veins shared with the arteries the same fibrovascular parenchyma between the bronchi. The cranial vein branches were in general more ventrally located with more branches draining the proximal and medial main CVB.

The first cranial trunk bifurcation was closest to the main pulmonary bifurcation on the left (Fig. 15B). The bifurcation created medial and dorsolateral branches. The dorsolateral branches in turn bifurcated into cranial and lateral branches. The medial branches bifurcated into additional medial and lateral branches. On the right, this medial branch became the DM*cr*CrT, while on the left it continued to the apex. The terminal apical vein on the right was derived from the lateral branch.

The remaining central medial pulmonary veins drained the ventromedial and pericardiac lung. The medial veins all arose from the caudal trunk on the right while on the left the DMcrCrT vein arose from the first lateral cranial trunk branch with the remaining medial veins branching from the caudal trunk.

The caudal pulmonary vein trunks branched into dorsomedial, dorsolateral, and lateral branches following the parenchymal divisions between the various CGBs (Fig. 15B).

J_ID: Z3X Customer A_ID: 11-0185.R1 Cadmus Art: AR22427 Date: 8-February-12 Stage: Page: 12

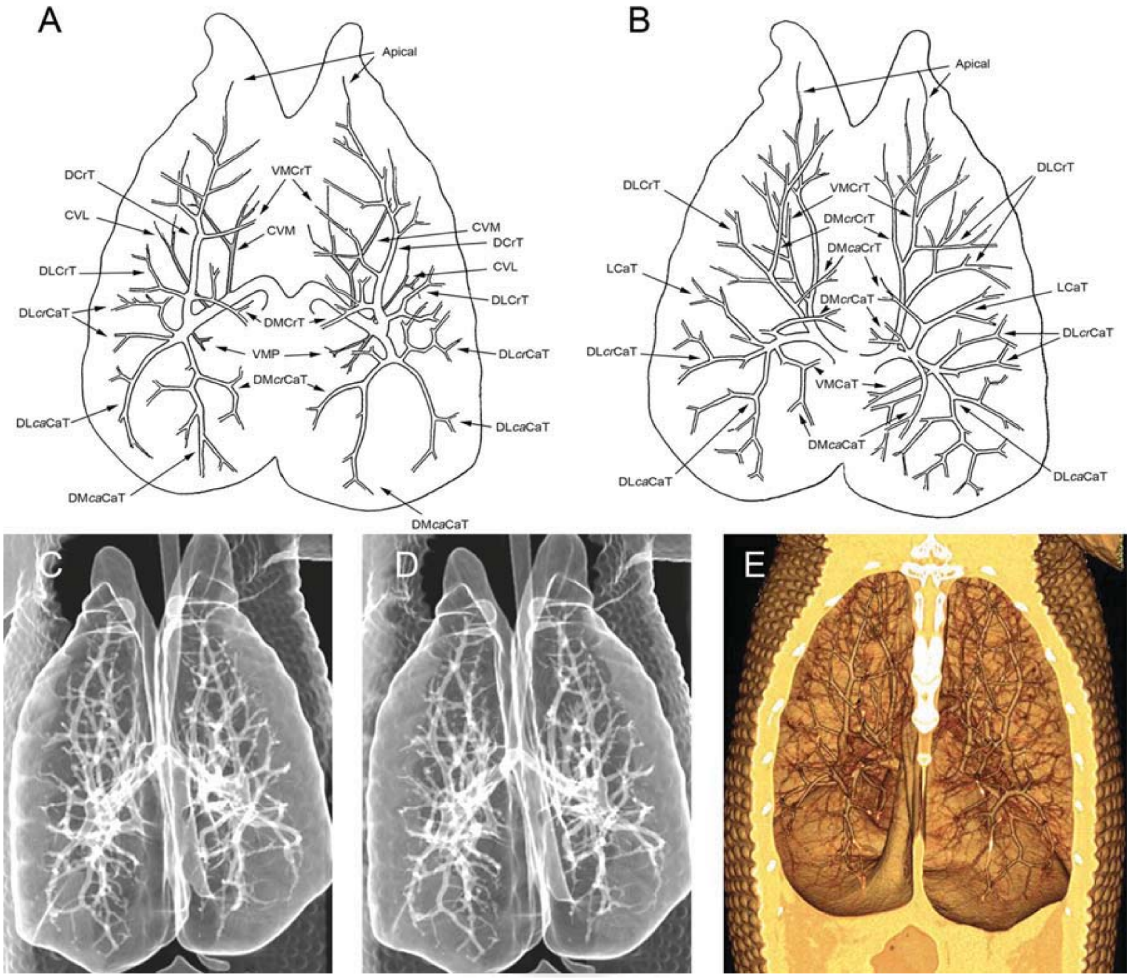

Fig. 15. Diagrammatic images in dorsal view of (**A**) the pulmonary arteries and (**B**) pulmonary veins that are based on conventional pulmonary arteriography and CT scan 3D reconstructions. Shaded vessels in (A) are more ventrally positioned. A semitransparent 3D airspace reconstruction stereo pair (**C**,**D**) and 3D surface volume rendering with dorsal cut away (**E**) are included to illustrate the challenges of interpreting the anatomy in three dimensions. Abbreviations: CVL—cranioventral lateral branch (br), CVM—cranioventral medial br., DCrT—dorsal br. cranial trunk (tr.), DLcaCaT—dorsolateral caudal br. caudal tr., DLcrCaT—dorsolateral cranial br. caudal tr., DLCrT—dorsolateral br. cranial tr., DMcaCaT—dorsomedial caudal br. caudal tr., DMcaCrT—dorsomedial caudal br. cranial tr., DMcrCaT—dorsomedial cranial br. caudal tr., DMCrT—dorsomedial br. cranial tr., DMcrCrT—dorsomedial cranial br. cranial tr., LCaT—lateral br. caudal tr., VMCaT—ventromedial caudal tr., VMCrT—ventromedial cranial tr., VMP—ventromedial pericardial br.

DISCUSSION

Critique of the Methods

Computed tomography is a powerful method to noninvasively study detailed anatomy but it has limitations that depend on resolution and software interpolations. In this study we use CT to map out the major branches of the conducting airways and the larger blood vessels. Subsequent reports will describe smaller airways and blood vessels, providing more detail on bronchial interconnections and their relationship to the capillary beds.

Functional Morphology of the Alligator Lung and Its Relationship With Other Crocodilians

Very little is known of the pulmonary anatomy of crocodilians. Several previous studies (Perry, 1988, 1989, 1990) described the gross anatomy and anatomical diffusion capacity of the Nile crocodile (*Crocodylus niloticus*). However, information on other crocodilian species is currently too scarce to allow comparisons that could establish the ground plan for the crown group, a group that includes the last common ancestor of the alligators, crocodiles, gharials, and which dates back to the Cretaceous Period (Brochu, 2003). Attempts to reconstruct the lung of this common ancestor are also confounded by unresolved phylogenetic relationships, particularly the relationship of the gharials, the relationships among caimans, and the relationships among crocodiles (Brochu, 2003). Although extant crocodilians all occupy a similar ecological niche (semiaquatic predator) and therefore share many features of their anatomy, such as a dorsoventrally flattened skull, short limbs relative to their body mass, and long and muscular tails, it is possible

ID: kalas | Black Lining: [ON] | Time: 14:01 | Path: N:/3b2/AR##/Vol00000/120027/APPFile/JW-AR##120027

details of their pulmonary anatomy differ across the Order Crocodylia, which consists of three Families (Alligatoridae, Gavialidae, Crocodilydae) containing eight genera. A description of one or two members of the Crocodylia is insufficient to distinguish synapomorphic from plesiomorphic features. Nevertheless, our study fills in some of the gaps in our knowledge and is helpful in sorting out relationships of the alligator lung with the avian respiratory system.

Our study of the lung of the American alligator reveals that it is much more birdlike than the previous recent descriptions of the Nile crocodile provided by Perry, and more consistent with Huxley's (1882) brief description of a crocodile (the species was not identified). Furthermore, our assessment is in keeping with recent physiological data of unidirectional airflow in alligator lungs (Farmer and Sanders, 2010). The relationship of the alligator secondary bronchi to each other and to the primary bronchus makes it clear how unidirectional airflow can occur in a birdlike manner whereas Perry concluded this phenomenon was not possible in the crocodile lung and that airflow was tidal. The structures Perry called chambers we have called secondary bronchi. On the basis of his studies of the Nile crocodile Perry stated that the caudal chambers arch caudally while the cranial chambers arch cranially and that this precludes direct caudocranial extrabronchial air circulation (Perry, 1992). He stated that there are only a scant few intercameral perforations connecting adjacent chambers that are "much too rare for such an important function" (Perry, 1992; p 160). Therefore Perry concluded that airflow was tidal. However, we do not find that the arrangement of the secondary bronchi of alligators matches this description of the crocodile lung. The alligator secondary bronchi are much more like the secondary bronchi of the avian lung (ventro- and dorsobronchi), discussed in detail below, in that numerous secondary bronchi (green, chartreuse, red, blue of Fig. 1) arch cranially. Connections between the secondary bronchi are not rare perforations, but regularly occurring tubular structures. Furthermore, although we find little evidence for mechanical valves, because of the acute angle the cervical ventral bronchus makes with the intrapulmonary bronchus, it is possible that an inspiratory aerodynamic valve is present at this location that functions very much like the avian valve, which is dependent on jetting phenomena (Banzett et al., 1987). Additionally, as noted above, the caudal ventrolateral lung is subdivided by numerous dissepiments into locules, each of which opens into the primary bronchus through a single ostium of small diameter. These ostia lie directly opposite the ostia to the caudal group bronchi. These structures may provide jets of air that entrain expiratory airflow into the dorsobronchal caudal group bronchi, and therefore play an avian like role in the expiratory aerodynamic valve.

Our assessment of the alligator pulmonary anatomy is similar to the crocodilian described by Huxley (1882), except Huxley reports more entobronchi and fewer ectobronchi than we find in the alligator. Although Huxley was primarily interested in the lung and body cavities of the kiwi, he noted the similarity of the kiwi lung with the crocodile lung. Huxley reported that the crocodile bronchus enters the lung and continues caudally as it dilates into an oval sac-like cavity that represents the mesobronchium and posterior air sac. He stated that the entobronchi of birds are represented in the five or six apertures on the dorsal and mesial walls of the mesobronchium that lead into canals. The cranial two pass directly cranially, the others lying more obliquely. The first canal is longest, largest, and dilates at the cranial end of the lung. It is connected to the second by transverse branches. The other two pass to the dorsal margin and lie superficially on the mesial face of the lung. Huxley also described four ventral chambers, the cranial two communicating with the entobronchi and the caudal two communicating with the mesobronchium. Two very large apertures in the dorsal wall of the mesobronchium gave rise to two very large canals, the ectobronchi. Finally Huxley stated, "the surfaces of all these canals, except the anterior half of the mesobronchium, are thickly set, lead into depressions, which are often so deep as to become cylindrical passages, simulating the parabronchia of birds" (Huxely, 1882; p 569). Huxley concluded that, "there is a fundamental resemblance between the respiratory organs of birds and those of crocodiles, pointing to some common form (doubtless exemplified by some of the extinct Dinosauria), of which both are modifications." We agree with Huxley's point of view. Because birds and crocodilians occupy very different ecomorphological niches, the fundamental resemblance is probably a consequence of shared ancestry rather than homoplasy arising from shared function. Developmental studies have provided much insight into deep homologies of other organ systems (Pichaud and Desplan, 2002), and therefore we have considered developmental data in our effort to understand homologous structures in the archosaur respiratory system.

Avian and Alligator Respiratory Systems

In this section we integrate our results on the topography of the juvenile alligator lung with developmental data from both birds and alligators, as well as anatomical data of the adult structures of avian respiratory systems with the aim of identifying homologous features and gaining insight into the respiratory system of the common ancestor. We find the most apparent difference between these systems to be the presence of avian air sacs, while the pattern of the air conducting bronchi in birds and alligators is remarkably similar. An overarching issue is whether this difference is superficial or fundamental. That is, are the air sacs of birds *de novo* structures that are separate from the lung, an idea that is reinforced by lexicon, or are the air sacs a part of the avian lung so that the common perception that air sacs are separate structures is incorrect. The embryonic origin of avian air sacs supports the latter view, that they are part of the lung; the abdominal sac is a distal expansion of the primary bronchus while the others are expansions of the secondary bronchi (discussed in detail below). Thus the air sacs are intrapulmonary saccular regions, which are common in nonmammalian vertebrates. Furthermore, the total volume of the avian respiratory system is about the same as the volume of the alligator lung; both are $\sim$150 mL kg^{-1} (Farmer, 2006). Given the apparent selection to conserve this volume to body mass ratio and the phylogenetic relationship of the two clades, it is not surprising to see similar segmentation of the hypervascular and hypovascular

lung by a similar mechanism and homologous structures. As the hypervascular parenchyma of extant birds is much more densely packed and miniaturized compared to the crocodilian, as seen in the alligator, their hypovascular air sac system is consequently much more elaborate.

In general birds possess a series of air sacs: paired cervical, anterior thoracic, posterior thoracic, abdominal, and a single interclavicular sac (Duncker, 1971). The cervical and interclavicular sacs occupy the cranial thoracic cavity and are proposed by Duncker (1971) to form a united functional entity such that in species with large cervical sacs the interclavicular is generally reduced and vice versa. These three sacs and the anterior thoracic sacs are all associated with entobronchi (ventrobronchi). The posterior thoracic sacs are associated with the laterobronchi (lateroventrobronchi) and the abdominal sacs are associated with the primary bronchi.

Previously Perry (1992) based on Moser (1904) proposed that the cranial sac-like dilation of the first lateral chamber of the crocodile is homologous with the avian interclavicular air sac (clavicular) and that the terminal chamber of the crocodile is homologous to the avian abdominal sac. Perry furthermore noted the following similarities of the structural plan of crocodilian and avian lungs, "(1) Cranially four groups of monopodally branching, tubular chambers (medioventral bronchi; parabronchi in birds); (2) caudally, numerous groups of arching, tubular chambers (mediodorsal bronchi; parabronchi in birds); and (3) anastomoses where the chambers meet: parabronchial anastomoses in the avian paleopulmo; intercameral perforations in the crocodile" (Perry, 1992; p 160). Thus Perry does not specifically homologize the cervical air sac, the anterior thoracic sac, the posterior thoracic sac, or the laterobronchi. On the basis of our study of the topography of juvenile alligator lungs, and on developmental data of both birds and alligators, we hypothesize a more complicated and more complete set of homologies. We suggest that structures of the juvenile alligator lung are better homologized with embryonic avian features than with the adult bird lung and therefore a brief discussion of avian and alligator development is germane and essential to make the case for the homologies. Therefore, we highlight a few key events during the development of the avian and alligator lung.

At Day 5.5, the chicken lung consists of a simple unbranched tube, the anlagen of the primary bronchus. This tube undergoes a spindle-shaped expansion at about two-fifths the length of the tube; the enlarged region is referred to by Locy and Larsel (1916) as the embryonic vestibulum. This swelling divides the primary bronchial anlagen into three regions, a proximal or interior, a middle region where the expansion is greatest, and a distal region (Locy and Larsell, 1916). Shortly after the appearance of the spindle-shaped expansion, buds arise from the primary bronchial anlagen. The first four buds to form arise from the dorsomesial aspect in the proximal or interior region of the primary bronchial anlagen (Fig. 16A); they are saccular with a narrow neck, curve dorsally and laterally around the primary bronchus, and grow to occupy the cranioventral region of the lung to give rise to the entobronchi (ventrobronchi). Although chickens have four entobronchi, this number varies with species to as many as six (Locy and Larsell,

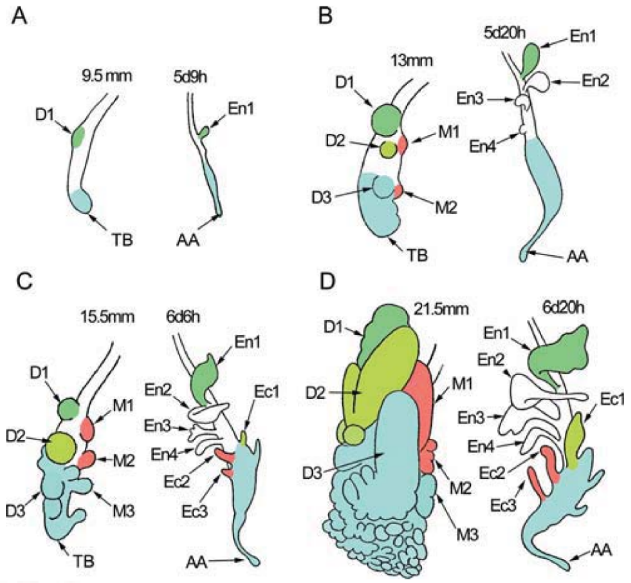

Fig. 16. Diagrammatic images of the left lung of an alligator at various embryonic lengths and the right embryonic chicken lung, in dorsal view, at various stages of development as indicated by days and hours after laying. (**A–D**) represent similar stages of development. Redrawn from Locy and Larsel (1916) and Broman (1941). Color coding indicates proposed homologies and correlates with the adult alligator pulmonary structures as depicted in Fig. 1 (CVB = green, DLB = chartreuse, DMBs = red, CGBs = light blue). Abbreviations: AA—abdominal air sac, D—numbered dorsal buds, Ec—numbered ectobronchi, En—numbered entobronchi, L—numbered laterobronchi, M—numbered medial buds, TB—terminal bud.

1916a; Duncker, 1971). The most proximal and first entobronchus to form subsequent branches to give rise to the cervical air sac and a portion of the interclavicular air sac, the lateral moiety of the interclavicular sac (Locy and Larsel, 1916a). The diameter of the first entobronchus widens considerably, and in the adults of some species the diameter exceeds by many fold the diameter of the primary bronchus (Duncker, 1971). Generally, the third entobronchus also subsequently branches to give rise to part of the interclavicular air sac, the mesial moiety, and the cranial (anterior) thoracic sac. After the four entobronchial buds are well established, another bud forms in the middle region of the primary bronchus. This bud gives rise to the first ectobronchus (dorsobronchus), which grows to a considerable length before the subsequent ectobronchial buds are more than papilla. A total of six or seven ectobronchi form in the chicken, but this number also varies depending on species and is nine in some (Locy and Larsell, 1916a; Duncker, 1971). None of the ectobronchi have direct connections to air sacs. At about the same time that the ectobronchial buds appear, six lateral buds form giving rise to the laterobronchi. The third laterobronchus expands to form the posterior thoracic air sac and the distal portion of the primary bronchial anlagen expands to form the abdominal air sac.

As in birds, in the early stages of development of the alligator lung there is an unbranched tube that develops a saccular expansion to partition the primary bronchial anlagen into three portions (Broman, 1940; Fig. 16B).

Buds arise on the primary bronchial anlagen that give rise to secondary bronchi. We hypothesize that the first and most proximal bud to form is homologous with the first avian entobronchus. This bud is referred to as D1 by Broman (1940). It is similar to the first avian entobronchus in that it arises in the proximal portion of the central lung tube in a region that does not undergo the large saccular expansion (Broman, 1940). Furthermore it branches in a manner that is reminiscent of the branching of the avian first entobronchus to form the cervical air sac and the lateral moiety of the interclavicular sac. It is also birdlike in that this secondary bronchus and its branches come to occupy the ventrocranial region of the lung (green cervical ventral bronchi of Fig. 1). It increases in diameter so that it is larger than any of the other bronchi and many fold larger than the primary bronchus. Finally, the pattern of airflow in this bronchus is birdlike in moving from a cranial toward a caudal direction (Farmer, 2010). In summary, we hypothesize that the alligator cervical ventral bronchus and its side branches are the homologues of the embryonic avian cervical air sac; the first entobronchus, and the lateral moiety of the interclavicular sac, which in the adult makes up only a portion of the whole interclavicular sac.

We furthermore hypothesize that the second dorsal bud to form in the alligator lung (DII of Broman 1940), which we believe is the same structure as our chartreuse dorsolateral bronchus (Fig. 1), is homologous to the first avian ectobronchus (dorsobronchus). This alligator airway is similar to the avian first ectobronchus in that it grows out of the region of the central lung tube that has undergone the saccular expansion and it grows in length greatly before any subsequent buds are more than papilla (Broman, 1940). It takes a dorsal course and then curves cranially (chartreuse DLB of Fig. 1) to overlie the entobronchus.

After DII has elongated, the subsequent dorsal buds form that take courses into what will become the hypervascular dorsal regions of the lung, and we therefore propose that they are homologous to the remaining avian ectobronchi. We believe DIII and DIV of Broman give rise to the lateral members of the caudal group bronchi (lateral blue caudal group bronchi of Fig. 1). The pattern of flow in the most cranial member of this group is the same as in the avian ectobronchi, from a caudal toward a cranial direction (Farmer, 2010). At approximately the same time as DIII and DIv are elongating, lateral and medial buds form. The medial buds grow dorsally into the region of the lung that will become well vascularized and appear to give rise to the dorsomedial bronchi (red DMBs of Fig. 1) and to the medial bronchi of the caudal group (blue CGMBs of Fig. 1). These might be homologues of avian ectobronchi however the latter (medial bronchi—red) are connections to hypovascular regions, and the embryonic chick ectobronchi do not connect to the air sacs. Therefore these could also be homologues of the entobronchi.

The ventrolateral buds are smaller and grow out to form numerous ventrolateral chambers that we hypothesize are homologous to the avian posterior thoracic sac. In the juvenile, the alligator caudal ventrolateral lung is subdivided by numerous dissepiments into locules with small diameter ostia into the primary bronchus. These ostia lie directly opposite the ostia to the CGBs. In aggregate, the locules line the entire ventrolateral lung caudal to the heart. There are two banks of locules extending caudally and roughly parallel to the posterior pericardial camera. The more medial of these appear to communicate with the posterior medial CGB and possibly the pericardial air sac associations with the DMcaB. Their primary communications are with their parent CGBs, with fewer terminal interconnections. The lateral bank camerae open toward the lateral members of the CGB. On the basis of the location and the developmental origins, we homologize these structures with the lateral bronchi and posterior thoracic air sacs. The alligator terminal bud seems clearly homologous to the abdominal air sac.

Alligator homologies to the entobronchial connections to the anterior thoracic air sac and the mesial moiety of the interclavicular sac are not clear. These connections are not as well conserved in birds and the variability may indicate these regions of the lung are under "relaxed" selection. As previously stated, in chickens these connections generally occur through the third entobronchus but in some individuals they occur through the second entobronchus. Furthermore, there is species variation with some taxa showing direct connections to the interclavicular sac from the primary bronchus (Duncker, 1971). Broman (1941) also reported that development of the caiman lung differs from that of the alligator, but offered few details of exactly how they differ. Thus, until additional developmental data are gathered, it is difficult to ascertain homologies in this region of the lung. However it is clear that the alligator cardiac lobes, or pericardial air sacs, contact the pericardial mediastinum and include dorsal pericardial air sacs that are associated with the medial proximal primary bronchus. They are in the right topographical location to be homologous with the avian mesial moiety of the interclavicular air sac. These air sacs partially encircle the anterior primary bronchus along with the more laterally positioned lateral moiety (Fig. 12A–D). The more caudal portion of the cardiac lobes appear homologous to the anterior thoracic sacs.

In summary, the lungs of juvenile alligators have a striking resemblance to the lung/air sac system of embryonic birds. A plausible explanation for this similarity is their shared ancestry, given the distinctly different life-history strategies of the extant lineages. More work is needed to refute or corroborate this hypothesis. Additional developmental, morphological, and physiological data are needed on a broader range of birds and crocodilians. However, if future data support our hypothesized homologies, then this study has helped remove the shroud of uncertainty that has obscured the form and function of the respiratory system of the Early Triassic animal that gave rise to the great archosaur radiation.

ACKNOWLEDGEMENTS

The authors thank The University of Utah School of Medicine and University Hospital for accommodating the research in providing access to their CT imaging facilities, and for the kind and expert care provided by the technical staff in obtaining the image data. They also thank Dr. Emma Schachner for assistance with the images and comments that greatly improved the quality of the manuscript. They also thank Dr. Andrew

Anderson and the University of Utah Department of Orthopedics Research Division for access to their computer lab and Dr. Anderson's endless patience in the instruction of using AMIRA. They thank Dr. Ruth Elsie and the Rockefeller Wildlife Refuge for providing the animals used in this research.

LITERATURE CITED

Banzett RB, Butler JP, Nations CS, Barnas JL, Lehr J, Jones JH. 1987. Inspiratory aerodynamic valving in goose lungs depends on gas density and velocity. Respir Physiol 70.

Benton MJ. 2004. Origin and relationships of dinosauria. In: Weishampel DB, Dodson P, Osmolska H, editors. The dinosauria. Berkeley: University of California Press. p 7–19.

Boelert R. 1942. Sur la physiologie de la respirataion de l' *Alligator mississippiensis*. Arch Int Physiol 52:57–72.

Brochu CA. 2003. Phylogenetic approaches toward crocodylian history. Annu Rev Earth Planetary Sci 31:357–397.

Broman I. 1939. Die Embryonalentwicklung der Lungen bei Krokedilen und Seeschildkröten. Z Mikrosk Anat Forsch 84:224–306.

Broman I. 1940. Die Embryonalentwicklung der Lungen bei Krokodilen und Seeschildkroten. Gegenbaurs Morphol Jahrbuch 1940: 244–306.

Brusatte SL, Benton MJ, Desojo JB, Langer MC. 2010. The higher-level phylogeny of Archosauria (Tetrapoda: Diapsida). Systematic Paleontol 8:3–47.

Brusatte SL, Benton MJ, Ruta M, Lloyd GT. 2008. Superiority, competition, and opportunism in the evolutionary radiation of dinosaurs. Science 321:1485–1488.

Carrier DR, Farmer CG. 2000. The evolution of pelvic aspiration in archosaurs. Paleobiology 26:271–293.

Duncker HR. 1971. The lung air sac system of birds. A contribution to the functional anatomy of the respiratory apparatus. Ergebn Anat EntwGesch 45:1–171.

Farmer CG. 1999. The evolution of the vertebrate cardio-pulmonary system. Annu Rev Physiol 61:573–592.

Farmer CG. 2000. Parental care: the key to understanding endothermy and other convergent features in birds and mammals. Am Nat 155:326–334.

Farmer CG. 2001. Parental care: a new perspective on the origin of endothermy. In: Gauthier JA, Gall LF, editors. New perspectives on the origin and early evolution of birds: Proceedings of the International Symposium in Honor of John H. Ostrom. New Haven: Peabody Museum of Natural History, Yale University. p 389–412.

Farmer CG. 2003. Reproduction, the selective benefit of endothermy. Am Nat 162:826–840.

Farmer CG. 2006. On the origin of avian air sacs. Respir Physiol Neurobiol 154:89–106.

Farmer CG. 2010. The provenance of alveolar and parabronchial lungs: insights from paleoecology and the discovery of cardiogenic, unidirectional airflow in the American alligator (*Alligator mississippiensis*). Physiol Biochem Zool 83:561–575.

Farmer CG, Carrier DR. 2000. Ventilation and gas exchange during treadmill-locomotion in the American Alligator (*Alligator mississippiensis*). J Exp Biol 203:1671–1678.

Farmer CG, Sanders K. 2010. Unidirectional airflow in the lungs of alligators. Science 327:338–340.

Hazelhoff EH. 1951. Structure and function of the lung of birds. Poultry Sci 30:3–10.

Holmes EB. 1975. A reconsideration of the phylogeny of the tetrapod heart. J Morphol 147:209–228.

Huxley TH. 1882. On the respiratory organs of *Apteryx*. Proc Zool Soc Lond 1882:560–569.

Locy WA, Larsell O. 1916. The embryology of the bird's lung based on observations of the domestic fowl Part I. Am J Anat 19: 447–506.

Maina JN. 2000. What it takes to fly: the structural and functional respiratory refinements in birds and bats. J Exp Biol 203: 3045–3064.

Maina JN. 2006. Development, structure, and function of a novel respiratory organ, the lung-air sac system of birds: to go where no other vertebrate has gone. Biol Rev 81:545–579.

Moser F. 1902. Beiträge zur vergleichenden Entwicklungsgeschichte der Wirbeltierlunge. Arch Mikrosk Anat Entwicklungsmech 60: 587–668.

Nesbitt SJ. 2011. The early evolution of archosaurs: relationships and the origin of major clades'. Bull Am Museum Nat Hist 352: 1–292.

Nesbitt SJ, Norell MA. 2006. Extreme convergence in the body plans of an early suchian (Archosauria) and ornithomimid dinosaurs (Theropoda). Proc R Soc Lond B 273:1045–1048.

Perry SF. 1988. Functional morphology of the lungs of the nile crocodile, *Crocodylus niloticus*: nonrespiratory parameters. J Exp Biol 134:99–117.

Perry SF. 1989. Morphology of crocodilian lungs. Fortschr Zool 35: 456–549.

Perry SF. 1990. Gas exchange strategy in the Nile crocodile: a morphometric study. J Comp Physiol B 159:761–769.

Perry SF. 1992. Gas exchange strategies of reptiles and the origin of the avian lung. In: Wood S, Weber R, Hargens A, Millard R, editors. Physiological adaptations in vertebrates: respiration, circulation, and metabolism. New York: Marcel Dekker. p 149–167.

Perry SF. 2001. Functional morphology of the reptilian and avian respiratory systems and its implications for theropod dinosaurs. In: Gauthier JA, Gall LF, editors. New perspectives on the origin and early evolution of birds: Proceedings of the International Symposium in Honor of John H. Ostrom. New Haven: Peabody Museum of Natural History, Yale University. p 429–441.

Pichaud F, Desplan C. 2002. Pax genes and eye organogenesis. Curr Opin Genet Dev 12:430–434.

Sereno PC. 1991. Basal archosaurs: Phylogenetic relationships and functional implications (Memoirs). J Vertebr Paleontol 11:1–53.

Seymour RS, Bennett-Stamper CL, Johnston SD, Carrier DR, Grigg GC. 2004. Evidence for endothermic ancestors of crocodiles at the stem of Archosaur evolution. Physiol Biochem Zool 77:1051–1067.

Wolf S. 1933. Zur kenntnis von Bau und Funktion der Reptilienlunge. Zool Jahrb Abt Anat Ontol 57:139–190.

AQ1: Please confirm that all author names are OK and are set with first name first, surname last.

AQ2: Kindly provide the volume or page numbers as appropriate for Banzett et al., 1987.